Study of freeze-out dynamics of strange hadrons

Sushant K. Singh,[1,2,*] Purabi Ghosh,[3,†] and Jajati K. Nayak[1,‡]
[1]*Variable Energy Cyclotron Centre, 1/AF, Bidhan Nagar, Kolkata-700064, India*
[2]*HBNI, Training School Complex, Anushakti Nagar, Mumbai 400085, India*
[3]*Dept. of Applied Physics and Ballistics, F. M. University, Balasore-756019, India*

(Received 22 April 2021; accepted 22 July 2021; published 26 August 2021)

We study the dynamics of chemical freeze-out of single strange hadrons—K, Λ, Σ, from a homogeneous and isotropically expanding system consisting of π, K, ρ, N, Λ, and Σ hadrons with zero net baryon density. We use the momentum-integrated Boltzmann equation or rate equation to study the evolution of strange hadrons considering Bjorken and Hubble-like expansions. We calculate the scattering rates of K, Λ, Σ and compare with the expansion rate to analyze the chemical freeze-out of these species. In this microscopic calculation the cross sections, which are input to the rate equation, are taken either from phenomenological models or are parametrized by comparing against experimental data. From this calculation it is found that these strange hadrons freeze out early near transition temperature T_c when the system follows a Hubble-like fast expansion. But, for a slower Bjorken-like expansion, strange hadrons take a longer time to decouple following a sequential behavior. The present calculation may set a guideline to understand the common freeze-out behavior of strange hadron species at Relativistic Heavy Ion Collider(RHIC) and Large Hadron Collider (LHC), which is mostly predicted by thermal models while explaining the yields of identified particles.

DOI: 10.1103/PhysRevD.104.034027

I. INTRODUCTION

Experimental observations and theoretical analysis suggest that quark gluon plasma (QGP)—one of the phases of quantum chromodynamics (QCD), is formed in relativistic heavy ion collisions at top RHIC and LHC energies [1–8]. The temperature and density of QGP is much higher compared to the normal nuclear matter. Once QGP is produced in such collisions it expands and undergoes a transition to hadronic matter, when the temperature of the system cools down to T_c. The system of interacting hadrons expands further with gradual fall in temperature and that leads to the decoupling of various hadronic species. At the decoupling, which is popularly called freeze-out, the particles stop interacting. Two types of decoupling, chemical and kinetic freeze-out, are realized in relativistic heavy ion collisions. In case of "chemical freeze-out" the inelastic scatterings between different hadronic species stop completely, whereas, in case of "kinetic freeze-out," the elastic scatterings stop and particles then follow a free-streaming motion. Corresponding temperatures are referred to in this article as T_{ch} and T_k, respectively. In such an expanding system the freeze-out is mostly decided by the scattering rates of interacting species and expansion rate of the system.

It has been a long-standing issue to analyze with rigor whether all hadron species decouple at the same time/temperature in an expanding system or if they do gradually at different times/temperatures. It is intuitive that different particle species decouple from the medium at different temperatures as their masses and interaction cross sections are different. But the models that explain experimental data observed from RHIC or LHC show that the decoupling of hadrons is consistent with a single freeze-out scenario at T_c [9–14]. Some models also explain the same data with a double freeze-out scenario [15,16]. Hence a detailed calculation in this regard is missing. Thus it is worth to study the freeze-out behavior of various species in different systems, more specifically in systems produced at RHIC and LHC energies. Again, the study at these energies may help in summarizing the properties of QCD matter and mapping some portion of QCD phase diagram.

The scenario where different species decouple gradually at different temperatures or times is referred to as sequential freeze-out. On the other hand, when they decouple at the same temperature, the scenario is termed simultaneous or common freeze-out. Theoretically, the mean-free paths of all species together become too large compared to the system size at simultaneous freeze-out. Some people also term it common universal freeze-out [17]. Both sequential and simultaneous nature of decoupling are plausible in case of chemical as well as kinetic freeze-outs in a multicomponent hadronic system.

*sushant7557@gmail.com
†purabi.bpd@gmail.com
‡jajati-quark@vecc.gov.in

Exact information on both chemical and kinetic freeze-outs of all species is highly important for hydrodynamic calculations. It has been observed that these calculations are somewhat successful in describing the hot and dense fluid produced at RHIC and LHC. But, we know most of these calculations [18–26] available for different observables such as net yield of identified hadrons, electromagnetic spectra, flow of the different species, etc., assume a simultaneous and sudden freeze-out scenario (both for T_{ch} and T_k) and attempt to provide important thermodynamic information of the produced system. The Cooper-Frye prescription is also employed with similar assumption of "sudden kinetic freeze-out (T_k)," which considers that the mean-free paths of the various hadron species become large enough suddenly through a thin freeze-out hypersurface. In hybrid model calculations, chemical freeze-out temperatures for all species are also assumed to be the same. T_c is chosen conveniently as T_{ch} to stop hydrodynamic evolution of the fluid and to start transport calculation for different species.

It is well known that the invariant yields and other observables depend on T_{ch} and T_k substantially. Hence it is highly important to know the behavior of both freeze-outs and temperatures accurately in case of relativistic heavy ion collisions. Considering this pertinent issue, an attempt has been made here to understand whether the freeze-out is simultaneous or sequential. Again, can it be sudden or is it continuous, and how does expansion of the system play a role?

In this article, we focus only on the study of chemical freeze-out of strange hadrons K, Λ, Σ. The dynamics related to chemical freeze-out is complex in nature due to the lack of complete understanding of all interactions in a multicomponent hadronic fluid. A microscopic approach using the momentum-integrated Boltzmann equation or rate equation is followed with the available interaction channels to analyze the behavior. We follow a similar approach discussed in [27] to study the freeze-out of various species in case of early universe. The scattering rates (Γ) of the species of interest are calculated and compared with the expansion rate (H) of the system. The calculation is done by considering a slower Bjorken expansion and a faster Hubble-like expansion. Then the freeze-out of K, Λ and Σ is discussed by comparing these rates in both cases. The present calculation discusses whether the assumption of simultaneous freeze-out at top RHIC and LHC energies is plausible or not. We keep the discussion of kinetic freeze out for future work.

Some attempts were made earlier to study the freeze-out scenario in relativistic heavy ion collisions [16,17,28–35]. The authors in [28] study the successive kinetic freeze-out scenario in a Bjorken type of expansion, but not the chemical freeze-out. In [30] the authors describe the breakdown of hydrodynamics and freeze-out of particles through the Cooper-Frye prescription with the assumption of sudden transition of particles in the fluid element in perfect local thermal equilibrium, but do not discuss the details of freeze-out behavior. Authors in [16] assume double freeze-out scenario to explain the observables using the hadron resonance gas (HRG) model. Sequential freeze-out has also been advocated in [34] using lattice calculation. Authors in [36] explained the chemical freeze-out of a gas of octet of pseudo-scalar mesons from chiral perturbation theory. But the present approach to study chemical freeze-out of strange hadrons in a multicomponent hadronic fluid is different.

In this article, since we are dealing with chemical freeze-out, the equilibrium would mean as chemical equilibrium from next onwards. We mention thermodynamic or kinetic equilibrium explicitly if phenomena related to both appear anywhere. Similarly the scattering here is basically inelastic scattering.

In the next section we give a note on the chemical equilibrium and freeze-out scenario to set up the problem. In Sec. III we discuss the dynamics by setting up a rate equation with notations for a two-component π-K system and discuss the freeze-out of kaon. In Sec. IV, we consider the system with hadrons $\pi, K, \bar{K}, \rho, N, \Lambda, \Sigma$ and evaluate the scattering rates of K, Λ, Σ and compare with expansion rate of the system. We finally summarize in Sec. V.

II. CHEMICAL EQUILIBRIUM AND FREEZE-OUT

A system in complete thermodynamic equilibrium (chemical, mechanical, and kinetic) may remain in equilibrium forever as long as the system is static and isolated. If the system consists of multiple species with some in complete and others in partial equilibrium, then the species which are not in equilibrium would try to achieve it after certain time depending on their scattering rates. To make the statements more precise, consider an isolated system at fixed volume (V) and temperature (T) that consists of two types of particles X and Z. Let the possible reactions in the system be

$$XX \rightleftharpoons ZZ.$$

Chemical equilibrium is the state when the rates of forward and backward reactions are equal. Once chemical equilibrium is achieved, although the reactions proceed at equal rates in the forward and backward directions, there is no net change in the number of X and Z particles, i.e., at chemical equilibrium

$$\frac{dN_i}{dt} = 0, \qquad i = X, Z,$$

where N_i denotes the total number of ith species. Let N_i^{eq} denote the corresponding total number at chemical equilibrium. If one of the species, say X, is not in chemical equilibrium then N_X relaxes to its equilibrium value

according to the following rate equation (see [27] for the derivation):

$$\frac{dN_X}{dt} = -\bar{R}[N_X^2 - (N_X^{\rm eq})^2], \tag{1}$$

where $\bar{R}$ is a constant and is a measure of the probability of X undergoing chemical reactions per unit time and depends only on T. Since T is fixed here, both $\bar{R}$ and $N_X^{\rm eq}$ are independent of time. Now for small departure from equilibrium, N_X can be written as $N_X = N_X^{\rm eq} + \delta N_X$ such that $\delta N_X \ll N_X^{\rm eq}$. Substituting this in Eq. (1) and ignoring quadratic powers in δN_X, we get

$$\frac{d}{dt}(\delta N_X) = -2\bar{R}N_X^{\rm eq}\delta N_X \Rightarrow \delta N_X(t) \sim e^{-t/\tau_X},$$

where $\tau_X = \frac{1}{2\bar{R}N_X^{\rm eq}}$, which means any perturbation away from equilibrium relaxes to its equilibrium value on a timescale τ_X. If the system consists of more than two particles and is not in chemical equilibrium, then each species relaxes due to inelastic scatterings in various channels and the system always leads to chemical equilibrium. For example, consider a system consisting of X, Y, Z and let the possible reactions be

$$XX \rightleftharpoons ZZ, \qquad YY \rightleftharpoons ZZ.$$

Further assume that X, Y are not in chemical equilibrium but Z is in chemical equilibrium. Then the rate equations for X and Y become

$$\frac{dN_X}{dt} = -\bar{R}_X[N_X^2 - (N_X^{\rm eq})^2],$$
$$\frac{dN_Y}{dt} = -\bar{R}_Y[N_Y^2 - (N_Y^{\rm eq})^2].$$

Linearizing and solving the above equations, we get

$$\delta N_X(t) \sim e^{-t/\tau_X}, \qquad \delta N_Y(t) \sim e^{-t/\tau_Y},$$

where $\tau_X = \frac{1}{2\bar{R}_X N_X^{\rm eq}}$ and $\tau_Y = \frac{1}{2\bar{R}_Y N_Y^{\rm eq}}$. This means that species X and Y relax to chemical equilibrium on timescales τ_X and τ_Y, respectively, and the relaxation time of the whole system is $\tau = \max(\tau_X, \tau_Y)$.

However, the picture changes when the system is expanding, due to which volume will not be a constant but changes with time. As a result T will become a function of time and so are the quantities $\bar{R}$ and $N_X^{\rm eq}$ in Eq. (1). Let us again consider the example of a system with X and Z particles as discussed above. Now we allow the volume to expand. We are interested in the early and late time dynamics of Eq. (1) when $\bar{R}$ and $N_X^{\rm eq}$ are functions of time/temperature. Initially, if the system is not far from equilibrium then we can write $N_X = N_X^{\rm eq} + \Delta$ such that $\Delta \ll N_X^{\rm eq}$ and $\frac{d\Delta}{dt} \ll \frac{dN_X^{\rm eq}}{dt}$. Equation (1) becomes

$$\frac{dN_X^{\rm eq}}{dt} = -2\bar{R}N_X^{\rm eq}\Delta \Rightarrow \Delta = -\frac{1}{2\bar{R}}\frac{d}{dt}\ln N_X^{\rm eq} \tag{2}$$

As time progresses, $\bar{R}$ decreases; also the time derivative of $N_X^{\rm eq}$ is decreasing in the negative direction. So Δ increases with time and the system is driven further away from equilibrium. After certain time, say t_{ch}, Δ becomes comparable in magnitude to $N_X^{\rm eq}$ and Eq. (2) no longer holds. However, for late times, i.e., $t \gg t_{ch}$, Δ becomes so large that one can write $N_X = N_X^{\rm eq} + \Delta \approx \Delta$. In that case Eq. (1) becomes

$$\frac{d\Delta}{dt} \approx -\bar{R}\Delta^2. \tag{3}$$

Now if $\bar{R}$ decreases faster than $1/t$ then it can be argued that for $t \to \infty$, $\Delta \to \Delta_\infty$(constant). For example, let us say $\bar{R} \sim \frac{1}{t^\alpha}$ for $\alpha > 1$, then we have

$$\frac{d\Delta}{dt} = -\frac{\Delta^2}{t^\alpha}.$$

Integrating the above equation, we get

$$\Delta(t) = -\frac{t^\alpha(\alpha-1)}{t + ct^\alpha(\alpha-1)} \overset{t\to\infty}{\to} -\frac{1}{c} = \Delta_\infty,$$

where c is an integration constant. The above arguments indicate that an expanding system, even if it starts in equilibrium, falls out of equilibrium due to expansion, as a result of which the interparticle separation increases and interaction rate decreases. At very late times, the interactions rates fall to such an extent that it will not be possible to further change the numbers of individual species and total numbers then become constant. This is called the chemical freeze-out and the corresponding time (temperature) at which this is achieved is called chemical freeze-out time (temperature). The effect of rate of expansion is implicit in t_{ch}. For a fast expansion, Δ becomes comparable to $N^{\rm eq}$ in a very short time, say (t_{ch}^F); however, for a slower expansion it takes a longer time for Δ to become of the order of $N^{\rm eq}$ and hence $t_{ch}^F < t_{ch}^S$.

For an expanding system with more than two particle species a question arises: Is it possible that the species freeze out simultaneously in a multicomponent system? In a multicomponent system, a particular species may be involved in several inelastic reactions. If t_c denotes the time when temperature of the system becomes T_c, then in the time interval (t_c, t_{ch}) as the temperature falls, the reactions with higher threshold will freeze out first as the reacting species may not possess enough thermal energy to overcome the threshold. Let $T_{\rm chi}$ be the temperature at which

any of the inelastic processes stop first and this marks the beginning of the freeze-out of the species. It is difficult to know this temperature exactly, as the thermal tail of distribution function at any temperature can provide the required threshold. However, probabilities of such processes with higher threshold are very less at a temperature of our interest. As time progresses and temperature falls, more and more inelastic channels involving the species stop and mean-free path increase gradually. At certain temperature, $T_{\rm ch}$, when the system cannot provide the required threshold for all the inelastic channels related to that species, the mean-free path (considering inelastic cross sections) becomes much larger. Hence the entire process of chemical freeze-out happens in a temperature range $T_{\rm chi} - T_{\rm ch}$ continuously. This range must be different for different species. Thus a sequential nature is expected. However, simultaneous freeze-out may be realized for a case where the fluid expansion is very fast which decreases the number density to a low value in a very short time. Thereby, expansion plays a crucial role in the freeze-out. To quantify, we discuss scenarios with a slow (Bjorken) and a fast (Hubble) expansion.

In this work, we study a multicomponent hadronic system with strange hadrons K, Λ, Σ and nonstrange hadrons π, ρ, N. Strange hadrons are considered to be away from equilibrium and are governed by a transport equation similar to Eq. (1). Assuming nonstrange hadrons to be in complete equilibrium which provide a thermal background to the strange hadrons, the scattering rates of strange hadrons are evaluated and compared with the expansion rate. The present work is divided into two parts. First, a simple π-K system is studied in the next section and the scattering rate of K is calculated. The analysis will be very similar to the system of X and Z presented in this section. But, the purpose is to present the equation that we will solve numerically in the following section. Then, the system with $\pi, K, \bar{K}, \rho, N, \Lambda, \Sigma$ is studied in the second part in Sec. IV.

III. $\pi - K$ SYSTEM

We first consider a simpler system of only π and K mesons assuming $n_K = n_{\bar{K}}$ at all times. The only possible inelastic reactions in such a system are $\pi\pi \to K\bar{K}$ and $K\bar{K} \to \pi\pi$. Pion is assumed to provide the thermal background and K is out of equilibrium. Now to analyze the freeze-out, the momentum-integrated Boltzmann equation or chemical rate equation for K can be written following Ref. [27] as

$$\frac{dn_K}{dt} + \Gamma_e n_K = R^o_{\pi\pi\to K\bar{K}} n_\pi n_\pi - R^o_{K\bar{K}\to\pi\pi} n_K n_{\bar{K}}, \quad (4)$$

where $\Gamma_e = \frac{1}{V}\frac{dV}{dT}$ denotes the expansion rate of the system and $R^o_{ab\to cd}$ denotes the thermal reaction rate as defined in [37,38]:

$$R^o_{ab\to cd} \equiv \langle \sigma_{ab\to cd} v_{ab} \rangle = \int d^3p_1 d^3p_2 f_a^{\rm eq}(p_1) f_b^{\rm eq}(p_2) \sigma v_{ab}.$$

σ denotes the cross section for the reaction $ab \to cd$, $f_a^{\rm eq}, f_b^{\rm eq}$ denote the equilibrium distributions of a and b, respectively, and v_{ab} denotes the relative velocity (Møller velocity) and is given by

$$v = \frac{\sqrt{(p_a.p_b)^2 - m_a^2 m_b^2.}}{E_a E_b}$$

p, m, and E are the momentum, mass, and energy of the interacting particles.

If we assume classical Boltzmann statistics for all the particles then the thermal reaction rate can be written as [38,39]

$$R^o_{ab\to cd}(T) = \frac{T g_a g_b}{32\pi^4 n_a^{\rm eq}(T) n_b^{\rm eq}(T)} \int_{s_0}^{\infty} ds[s - (m_a + m_b)^2] \times [s - (m_a - m_b)^2] \frac{\sigma(s)}{\sqrt{s}} K_1(\sqrt{s}/T), \quad (5)$$

where $\sqrt{s_0} = \max(m_a + m_b, m_c + m_d)$ and s is the square of the center of mass energy. In absence of the expansion term, equilibrium condition demands that we must have

$$R^o_{\pi\pi\to K\bar{K}} n_\pi^{\rm eq} n_\pi^{\rm eq} = R^o_{K\bar{K}\to\pi\pi} n_K^{\rm eq} n_{\bar{K},}^{\rm eq}$$

and since we assume π's to be always in equilibrium, hence the rate equation becomes

$$\frac{dn_K}{dt} + \Gamma_e n_K = R^o_{K\bar{K}\to\pi\pi}[n_K^{\rm eq} n_{\bar{K}}^{\rm eq} - n_K n_{\bar{K}}]. \quad (6)$$

Since $n_K = n_{\bar{K}}$, the above equation can also be written as

$$\frac{dn_K}{dt} + \Gamma_e n_K = R^o_{K\bar{K}\to\pi\pi}[(n_K^{\rm eq})^2 - (n_K)^2]. \quad (7)$$

Following [27], we now define $Y_K = n_K/s$, where s is the entropy density, to scale out the effect of expansion, and $x = T_c/T$ which is a dimensionless quantity. Here $T_c = 155$ MeV is the crossover temperature at $\mu_B = 0$. $x = x_c = 1$ is then the point where we start the evolution for chemical rate equations. In the context of heavy ion collisions at $\mu_B = 0$, due to large abundance of pions, entropy is related to the yields of pions. Then Y_K is related to the ratio of kaons to pions yields. The lhs of Eq. (7) can be written as

$$\frac{dn_K}{dt} + \Gamma_e n_K = s\dot{Y}_K.$$

Also,

$$\dot{Y}_K = \frac{dx}{dt}\frac{dY_K}{dx} = -\frac{T_c}{T^2}\left(\frac{dT}{dt}\right)\frac{dY_K}{dx} = -\frac{x^2}{T_c}\left(\frac{dT}{dt}\right)\frac{dY_K}{dx.}$$

Hence, the rate equation (7) becomes

$$\frac{dY_K}{dx} = -\frac{T_c s}{x^2}\left(\frac{dT}{dt}\right)^{-1} R^o_{K\bar{K}\to\pi\pi}[(Y_K^{\rm eq})^2 - (Y_K)^2]. \quad (8)$$

Other inputs that are needed to solve Eq. (8) are s, dT/dt, and Γ_e. To obtain s, one should in principle calculate the entropy density of an interacting pion gas. However, such a calculation is beyond the scope of this work. In the temperature range in which we are interested ($T < 155$ MeV), due to low mass, pions are the most abundant species. So in this temperature range, the entropy density of a pure pion gas should not differ much from the entropy density of a gas of hadrons for which parametrization are available in the literature. So in this and the later section, to a first approximation, we use the parametrization from [40] for pressure (P) obtained using the results from the lattice QCD and HRG model and is given by

$$\frac{P(T)}{T^4} = \frac{a_0 + a_1/t + a_2/t^2 + a_3/t^3 + a_4/t^4 + a_5/t^5}{b_0 + b_1/t + b_2/t^2 + b_3/t^3 + b_4/t^4 + b_5/t^5}, \quad (9)$$

with $t = T(\text{MeV})/154$. The values of parameters $a_i's$ and $b_i's$ are quoted in Ref. [40]. The entropy density and speed of sound (c_s^2) are then obtained using the following identities:

$$s(T) = \frac{dP}{dT}, \qquad \frac{1}{Tc_s^2(T)} = \frac{1}{s}\frac{ds}{dT}.$$

To find Γ_e, we study the system with a slow Bjorken (BJ) expansion and a faster Hubble-like (HB) expansion. For Bjorken expansion, the four-velocity is

$$u^\mu = \frac{t}{\tau}\left(1, 0, 0, \frac{z}{t}\right)$$

with $\tau = \sqrt{t^2 - z^2}$; using $\Gamma_e = \partial_\mu u^\mu$, one gets the expansion rate corresponding to Bjorken expansion as

$$\Gamma_e^B = \frac{1}{\tau}.$$

For Hubble-like expansion, the four-velocity

$$u^\mu = \frac{t}{\tau}\left(1, \frac{x}{t}, \frac{y}{t}, \frac{z}{t}\right),$$

with $\tau = \sqrt{t^2 - x^2 - y^2 - z^2}$. This leads to the following expansion:

$$\Gamma_e^H = \frac{3}{\tau.}$$

If the expansion is homogeneous and isotropic, then we can set $x = y = z = 0$ and get

$$\Gamma_e = \begin{cases} 1/t & \text{Bjorken flow (BJ)} \\ 3/t & \text{Hubble-like flow (HB)} \end{cases} \quad (10)$$

The temperature dependence of Γ_e can be obtained by assuming that the expansion is isentropic so that we have the following continuity equation:

$$\frac{ds}{dt} + \Gamma_e s = 0.$$

Using Eq. (10), s can be obtained as a function of t and gives $s \sim t^{-a}$, where $a = 1$ for BJ and $a = 3$ for HB expansion. Equivalently,

$$st^a = \text{constant}.$$

Hence $\Gamma_e = -\frac{1}{s}\frac{ds}{dt}$ will become

$$\Gamma_e = \frac{a}{(s_0/s)^{1/a} t_0}.$$

The temperature dependence of s will then give the temperature dependence to Γ_e. We choose $T_0 = 355$ MeV and $t_0 = 1$ fm as the initial temperature and thermalization time, respectively, of the QGP.

$\frac{dT}{dt}$ can be obtained with the help of s and Γ_e as follows:

$$\Gamma_e = -\frac{1}{s}\frac{ds}{dt} = -\frac{1}{s}\frac{ds}{dT}\frac{dT}{dt} = -\frac{1}{Tc_s^2}\frac{dT.}{dt}$$

Hence

$$\frac{dT}{dt} = -Tc_s^2\Gamma_e,$$

and the rate equation (8) becomes

$$\begin{aligned}\frac{dY_K}{dx} &= \frac{s}{xc_s^2\Gamma_e} R^o_{K\bar{K}\to\pi\pi}[(Y_K^{\rm eq})^2 - (Y_K)^2] \\ &= -\frac{Y_K^{\rm eq}}{x}\frac{sY_K^{\rm eq}}{c_s^2\Gamma_e} R^o_{K\bar{K}\to\pi\pi}\left[\frac{(Y_K)^2}{(Y_K^{\rm eq})^2} - 1\right] \\ &= -\frac{Y_K^{\rm eq}}{x}\frac{\Gamma}{H}\left[\frac{(Y_K)^2}{(Y_K^{\rm eq})^2} - 1\right], \end{aligned} \quad (11)$$

where $\Gamma = sY_K^{\rm eq} R^o_{K\bar{K}\to\pi\pi} = n_K^{\rm eq} R^o_{K\bar{K}\to\pi\pi}$ denotes the thermal rate at which kaons are annihilated and $H = c_s^2\Gamma_e = |\frac{1}{T}\frac{dT}{dt}|$ denotes the rate at which the system cools. Finally,

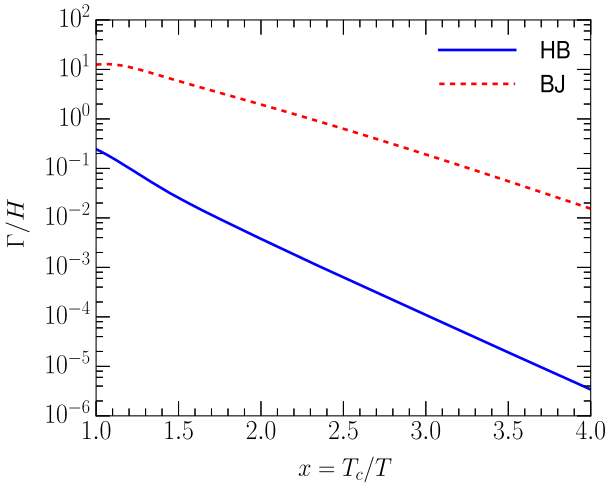

FIG. 1. The ratio of annihilation rate of kaons to cooling rate of the system, Γ/H plotted as a function of $x = T_c/T$ for Bjorken (BJ) and Hubble-like (HB) flows in a π-K system.

$$\frac{x}{Y_K^{\rm eq}}\frac{dY_K}{dx} = -\frac{\Gamma}{H}\left[\frac{(Y_K)^2}{(Y_K^{\rm eq})^2} - 1\right]. \tag{12}$$

The rate equation in the form given in Eq. (12) suggests that even if the system starts in equilibrium initially, i.e., at $x = 1$, it is driven out of equilibrium as x increases and the rate at which this happens is controlled by the factor Γ/H. The ratio, annihilation to expansion rate Γ/H for π-K system is shown in Fig. 1. The solid blue line represents the ratio when the system follows a Hubble-like expansion and the red dashed line represents the ratio when it follows Bjorken expansion. Since the Hubble expansion rate is larger, the ratio Γ/H is smaller and less than 1 during the entire evolution period. In case of the slower Bjorken expansion, the expansion rate is smaller and Γ/H is more than 1 at larger temperature. Then the system experiences less scatterings due to sufficient fall in temperature, leading to $\Gamma/H < 1$ beyond $x = 2.3$.

With the inputs explained above, we now numerically solve Eq. (8). The numerical solution is shown in Fig. 2 for both BJ and HB cases where we plot the logarithm of Y_K normalized to its initial value $Y_K^c = Y_K(x_c)$, (i.e., the value at $t = t_c$ or $x = 1$). And, the initial value is chosen to be the equilibrium value at T_c, i.e., $Y_K^c \equiv n_K^{\rm eq}(T_c)/s(T_c)$. We also show the evolution of equilibrium value $Y_K^{\rm eq} = n_K^{\rm eq}(T)/s(T)$ (normalized to Y_K^c) by the solid green line for a baseline to compare with the numerical results of Eq. (8).

As the evolution starts, the expansion drives the system away from equilibrium. But, the rate at which this happens depends on the expansion rate. In the BJ case, since the expansion rate is slower compared to the scattering one, the ratio Γ/H is greater than 1 and kaons remain close to equilibrium for a certain time. After which the departure from equilibrium becomes quite significant as the ratio Γ/H decreases. For sufficiently longer time, the ratio Γ/H becomes negligibly small, and Y_K does not change much and approaches a constant value which corresponds to freeze-out of kaons. As can be seen from Fig. 2, for the BJ case the net yield changes slowly and takes a longer time for the freeze-out process. This is because of the slow expansion in the case of Bjorken dynamics. On the other hand, for the HB case, the cooling rate is much faster so that the ratio Γ/H is negligibly small right from the beginning of the evolution. Hence, Y_K does not change much compared to its initial value as can be seen by the constant line (dashed-dotted blue) in Fig. 2. In other words, the yield does not change much compared to the initial value and gets frozen close to T_c. Freeze-out temperature is thus close to T_c.

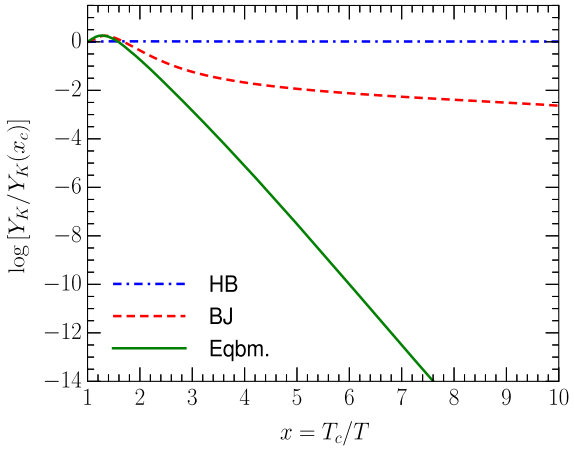

FIG. 2. Numerical solution of Eq. (8) with suitable normalization.

IV. $\pi - K - \rho - N - \Lambda - \Sigma$ SYSTEM

Now we consider a system consisting of $\pi, K, \bar{K}, \rho, N, \Lambda, \Sigma$. We assume that the nonstrange particles (π, ρ, N) provide a thermal background till the time of the freeze-out of the strange hadrons $(K, \bar{K}, \Lambda, \Sigma)$. The assumption of nonstrange hadrons providing a thermal background can be justified as follows: the nonstrange hadrons involve pions which are the lightest hadrons and are produced in large numbers compared to the strange hadrons. Also, πN cross sections are usually larger compared to meson-meson interactions and ρ-meson is a resonance state in the $\pi\pi$ scattering. Hence, the interaction rate among nonstrange hadrons at any time would be larger compared to strange hadrons so that they achieve equilibrium faster compared to strange hadrons. We employ the momentum-integrated Boltzmann equation or rate equations to study the dynamics. The details of the cross sections, which go as input in the rate equations, can be found in [41].

Considering all possible inelastic reactions and following the notations of the previous section, the evolution equations for $K, \bar{K}, \Lambda$, and Σ can be written as

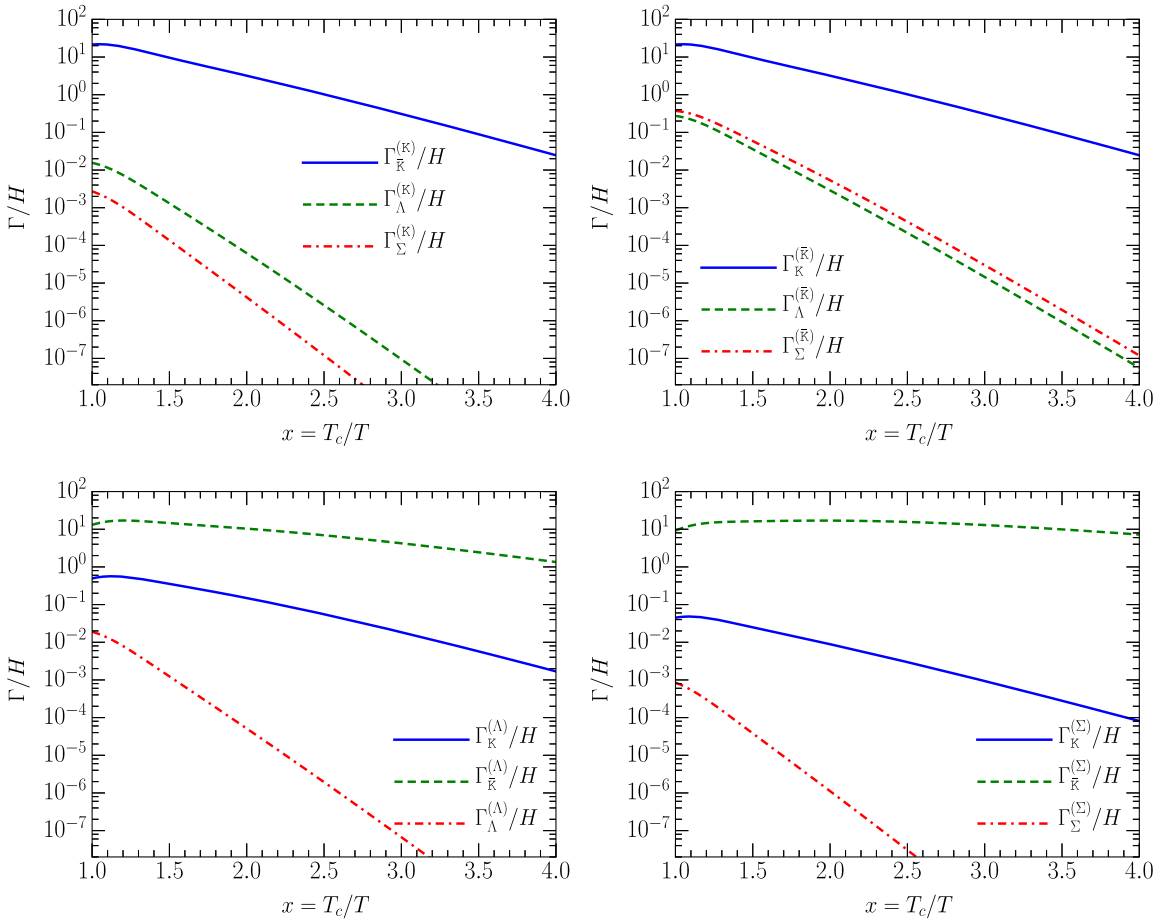

FIG. 3. Different rates appearing in Eqs. (13)–(16) for BJ case.

$$\frac{x}{Y_K^{\rm eq}}\frac{dY_K}{dx} = -\frac{\Gamma_{\bar{K}}^{(K)}}{H}\left[\frac{Y_K Y_{\bar{K}}}{Y_K^{\rm eq} Y_{\bar{K}}^{\rm eq}} - 1\right] - \frac{\Gamma_{\Lambda}^{(K)}}{H}\left[\frac{Y_K Y_\Lambda}{Y_K^{\rm eq} Y_\Lambda^{\rm eq}} - 1\right] - \frac{\Gamma_{\Sigma}^{(K)}}{H}\left[\frac{Y_K Y_\Sigma}{Y_K^{\rm eq} Y_\Sigma^{\rm eq}} - 1\right], \tag{13}$$

$$\frac{x}{Y_{\bar{K}}^{\rm eq}}\frac{dY_{\bar{K}}}{dx} = -\frac{\Gamma_{K}^{(\bar{K})}}{H}\left[\frac{Y_{\bar{K}} Y_K}{Y_{\bar{K}}^{\rm eq} Y_K^{\rm eq}} - 1\right] - \frac{\Gamma_{\Lambda}^{(\bar{K})}}{H}\left[\frac{Y_{\bar{K}}}{Y_{\bar{K}}^{\rm eq}} - \frac{Y_\Lambda}{Y_\Lambda^{\rm eq}}\right] - \frac{\Gamma_{\Sigma}^{(\bar{K})}}{H}\left[\frac{Y_{\bar{K}}}{Y_{\bar{K}}^{\rm eq}} - \frac{Y_\Sigma}{Y_\Sigma^{\rm eq}}\right], \tag{14}$$

$$\frac{x}{Y_\Lambda^{\rm eq}}\frac{dY_\Lambda}{dx} = -\frac{\Gamma_{K}^{(\Lambda)}}{H}\left[\frac{Y_\Lambda Y_K}{Y_\Lambda^{\rm eq} Y_K^{\rm eq}} - 1\right] - \frac{\Gamma_{\bar{K}}^{(\Lambda)}}{H}\left[\frac{Y_\Lambda}{Y_\Lambda^{\rm eq}} - \frac{Y_{\bar{K}}}{Y_{\bar{K}}^{\rm eq}}\right] - \frac{\Gamma_{\Lambda}^{(\Lambda)}}{H}\left[\frac{(Y_\Lambda)^2}{(Y_\Lambda^{\rm eq})^2} - 1\right], \tag{15}$$

$$\frac{x}{Y_\Sigma^{\rm eq}}\frac{dY_\Sigma}{dx} = -\frac{\Gamma_{K}^{(\Sigma)}}{H}\left[\frac{Y_\Sigma Y_K}{Y_\Sigma^{\rm eq} Y_K^{\rm eq}} - 1\right] - \frac{\Gamma_{\bar{K}}^{(\Sigma)}}{H}\left[\frac{Y_\Sigma}{Y_\Sigma^{\rm eq}} - \frac{Y_{\bar{K}}}{Y_{\bar{K}}^{\rm eq}}\right] - \frac{\Gamma_{\Sigma}^{(\Sigma)}}{H}\left[\frac{(Y_\Sigma)^2}{(Y_\Sigma^{\rm eq})^2} - 1\right], \tag{16}$$

where the scattering rates of various channels contributing to the net productions are defined as follows:

$$\begin{aligned}
\Gamma_{\bar{K}}^{(K)} &= n_{\bar{K}}^{\rm eq}[R^o_{K\bar{K}\to\pi\pi} + R^o_{K\bar{K}\to\pi\rho} + R^o_{K\bar{K}\to\rho\rho} + R^o_{K\bar{K}\to p\bar{p}}],\\
\Gamma_{\Lambda}^{(K)} &= n_{\Lambda}^{\rm eq}[R^o_{K\Lambda\to\pi N} + R^o_{K\Lambda\to\rho N}],\\
\Gamma_{\Sigma}^{(K)} &= n_{\Sigma}^{\rm eq} R^o_{K\Sigma\to\pi N},\\
\Gamma_{K}^{(\bar{K})} &= n_{K}^{\rm eq}[R^o_{K\bar{K}\to\pi\pi} + R^o_{K\bar{K}\to\pi\rho} + R^o_{K\bar{K}\to\rho\rho} + R^o_{K\bar{K}\to p\bar{p}}],\\
\Gamma_{\Lambda}^{(\bar{K})} &= n_{N}^{\rm eq} R^o_{\bar{K}N\to\Lambda\pi}, \qquad \Gamma_{\Sigma}^{(\bar{K})} = n_{N}^{\rm eq} R^o_{\bar{K}N\to\Sigma\pi},\\
\Gamma_{K}^{(\Lambda)} &= n_{K}^{\rm eq}[R^o_{\Lambda K\to\pi N} + R^o_{\Lambda K\to\rho N}],\\
\Gamma_{\bar{K}}^{(\Lambda)} &= n_{\pi}^{\rm eq} R^o_{\Lambda\pi\to\bar{K}N}, \qquad \Gamma_{\Lambda}^{(\Lambda)} = n_{\Lambda}^{\rm eq} R^o_{\Lambda\Lambda\to p\bar{p}}\\
\Gamma_{K}^{(\Sigma)} &= n_{K}^{\rm eq} R^o_{\Sigma K\to\pi N}, \qquad \Gamma_{\bar{K}}^{(\Sigma)} = n_{\pi}^{\rm eq} R^o_{\Sigma\pi\to\bar{K}N},\\
\Gamma_{\Sigma}^{(\Sigma)} &= n_{\Sigma}^{\rm eq} R^o_{\Sigma\bar{\Sigma}\to p\bar{p}}.
\end{aligned}$$

The above rates are plotted in Figs. 3 and 4. The cross sections for various hadronic processes producing hyperons and strange mesons are already mentioned in [41]. The cross sections of all inverse reactions are obtained using the principle of detailed balance as follows:

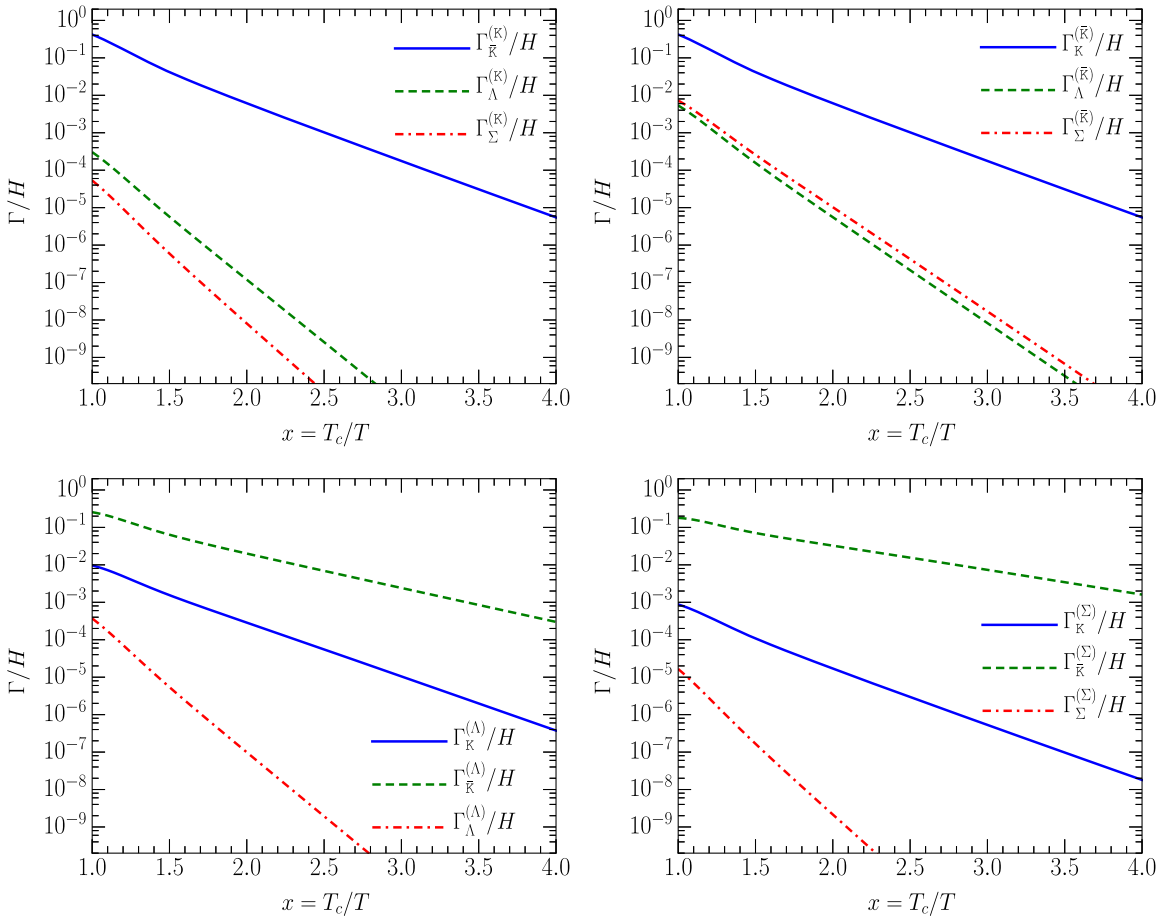

FIG. 4. Different rates appearing in Eqs. (13)–(16) for HB case.

$$\sigma_{f\to i} = \frac{{p_i}^2}{{p_f}^2}\frac{g_i}{g_f}\sigma_{i\to f}, \tag{17}$$

where p_i, p_f are, respectively, the center of mass momenta and g_i, g_f are the total degeneracies of the initial and final channels.

It can be observed that the ratio Γ/H is different for different channels. As a result, different channels should freeze out at different temperatures.

Now we solve the coupled differential equations Eqs. (13)–(16) numerically. The evolution starts at $T = T_c = 155$ MeV or $x = 1$. The initial number densities are chosen as the equilibrium values at T_c, i.e., $n_K^{(0)} \equiv n_K^{\rm eq}(T_c)$, $n_{\bar{K}}^{(0)} \equiv n_{\bar{K}}^{\rm eq}(T_c), n_\Lambda^{(0)} \equiv n_\Lambda^{\rm eq}(T_c), n_\Sigma^{(0)} \equiv n_\Sigma^{\rm eq}(T_c)$. The numerical solution is shown in Figs. 5 and 6. In the present calculation, the freeze-out is achieved when the variable $Y_i = n_i/s$ saturates. It comes automatically when $1/\langle n\sigma v\rangle$ (scattering information from microscopic inputs) becomes small compared to $\tau_{\rm exp}$ (system expansion).

In the left panel of Fig. 5 the solution is plotted for the BJ case and in the right panel for the HB case. Figure 6 shows a comparative plot for Λ yield for both BJ and HB cases. For the BJ case, K and $\bar{K}$ decouple at later time (or lower temperature) whereas Λ and Σ decouple earlier (or higher temperature). For the HB case, since the expansion rate is larger, all channels freeze out as soon as the evolution starts so that the yields of all the particles are fixed at $T \approx T_c$ (the yield however changes by about 2% for K, $\bar{K}$ and about 6% for Λ, Σ); hence, the chemical freeze-out temperature for all is $T_{\rm ch} \approx T_c$. But if one observes, the value of yields of different species are fixed at different temperatures although close to T_c. Again, it is prominent if one starts with initial densities little away from equilibrium values.

With different initial number densities the yields of K, Λ are plotted in Figs. 7 and 8. We have already discussed the evolution of the strange species when they start evolving with equilibrium initial densities at T_c and have shown how they decouple as expansion continues. In Figs. 7 and 8, the results of Eqs. (13) and (15) with initial densities $n^i \neq n^{eq}$ are shown for K, Λ for both cases of Bjorken and Hubble expansion, respectively. All the curves with black color (online) represent the evolution of K and with blue color (online) represent the evolution of Λ. Solid lines are for $n^i = n^{eq}$, dashed lines are the solution with $n^i = 0.85n^{eq}$, and dotted lines for $n^i = 0.75n^{eq}$. The qualitative trend of the evolution with $n^i \neq n^{eq}$ is the same as $n^i = n^{eq}$. When the system starts with initial condition slightly away from

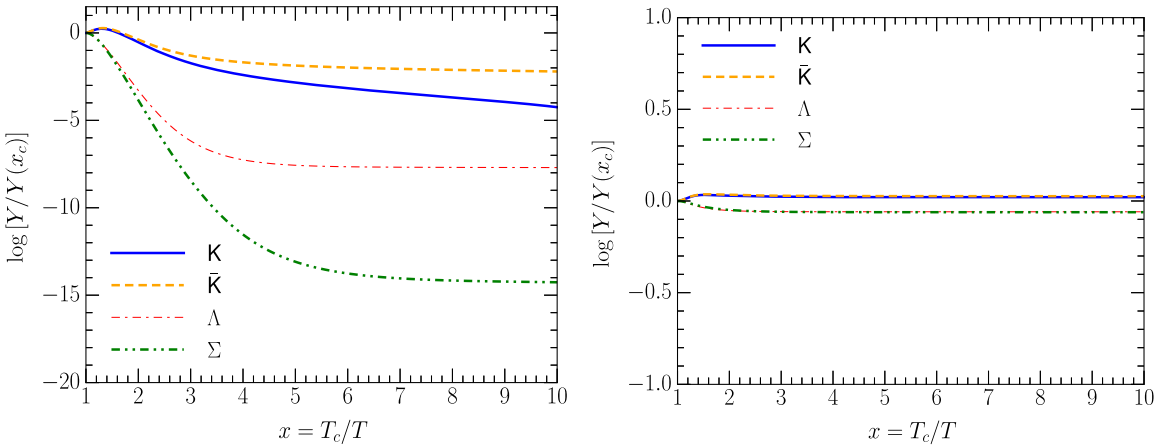

FIG. 5. Numerical solution of Eqs. (13)–(16) (left panel) BJ case and (right panel) HB case.

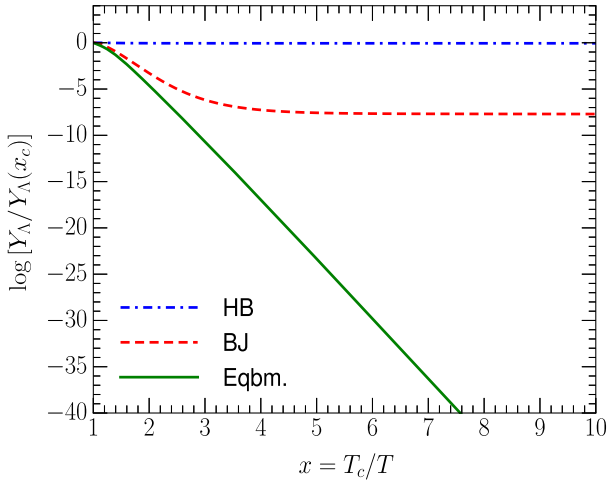

FIG. 6. Numerical solution of Eq. (15) with suitable normalization.

equilibrium value, interactions try to maintain the equilibrium. Gradually with expansion, when the density/temperature becomes insufficient for an inelastic collision, species decouple; $Log(Y/Y(x_c))$ saturates. From Fig. 8 it is found that change in the Λ yield with $n^i = 0.85n^{eq}$ or $0.75n^{eq}$ does not differ much from the yield with $n^i = n^{eq}$ in case of Hubble expansion, whereas the distinction is prominent for K yield. Actually there is a difference, but it is small compared to the case of Bjorken expansion. Difference is visible when the scale is changed. The difference in yield of Λ with $n^i = 0.75n^{eq}$ and $n^i = n^{eq}$, for the case of Hubble expansion, is small because the yield saturates soon or decoupling happens early during evolution. In case of Bjorken, the yield saturates later and by that time the difference in yield (for $n^i = n^{eq}$ from $n^i = 0.85n^{eq}$ or $0.75n^{eq}$) grows because of the secondary interaction.

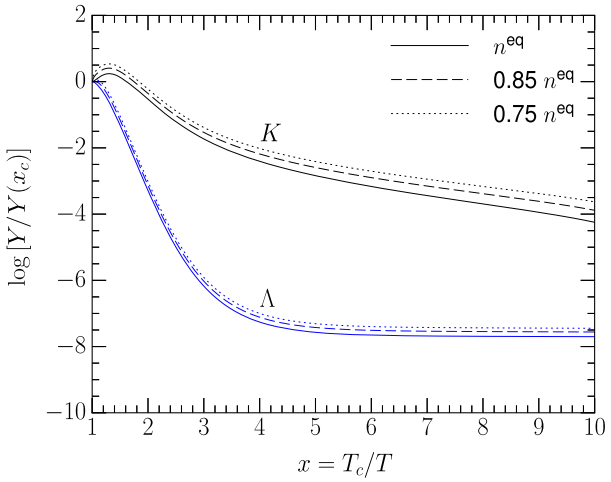

FIG. 7. K and Λ yields are plotted considering initial densities $n = 0.85n_{eq}$ and $n = 0.75n_{eq}$ when system follows Bjorken expansion. These are the solution of Eqs. (13) and (15) with suitable normalization.

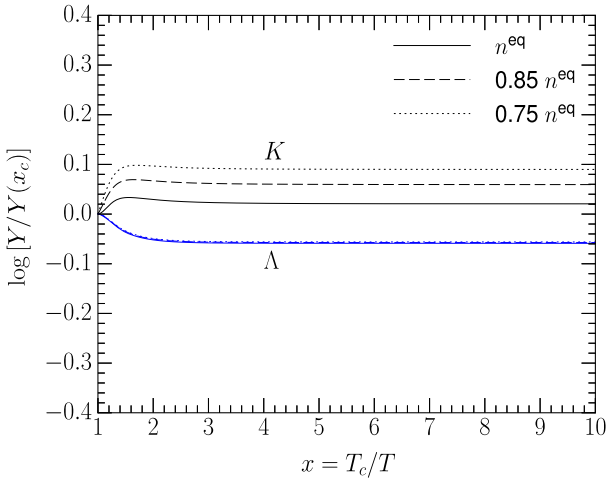

FIG. 8. K and Λ yields are plotted considering initial densities $n = 0.85n_{eq}$ and $n = 0.75n_{eq}$ when system follows Hubble expansion. These are the solution of Eqs. (13) and (15) with suitable normalization.

V. SUMMARY AND CONCLUSIONS

Hydrodynamics along with transport calculation provide a comprehensive model to describe the matter created at top RHIC and LHC energies. But, these calculations require information of freeze-out temperature(s) along with initial thermalization and transition temperatures to infer accurate properties. Hence it is important to know the freeze-out temperature(s) at which different species decouple chemically as has been highlighted in this paper. In this work a microscopic analysis is carried out to understand the *chemical freeze-out* behavior of single strange hadrons K, Λ, and Σ assuming a homogeneous and isotropically expanding hadronic system consisting of π, K, ρ, N, Λ, and Σ at zero net baryon density.

The study is made for two scenarios; i.e., part I is described in Sec. III and part II is described in Sec. IV. The description of part I in Sec. III is about the freeze-out of kaons in an expanding π-K system, where the rate equation or momentum-integrated Boltzmann equation has been used to study the evolution of kaons. The scattering rates are evaluated and compared with the expansion rate considering both Bjorken and Hubble-like expansions. It is observed that the expansion dynamics plays a major role and the kaons take longer time to freeze out when the system follows Bjorken expansion. However, for the system following Hubble expansion, kaon yield gets frozen early around T_c. The calculation is then extended(part II in Sec. IV), to study the freeze-out of K, Λ, and Σ in a hadronic system with $\pi, \rho, K, \bar{K}, N, \Lambda, \Sigma$ as constituents which is described in Sec. IV. Similar observations of late freeze-out of strange hadrons in case of Bjorken expansion and an early freeze-out near T_c in case of Hubble-like expansion are obtained. In addition, it is observed that the single strange hadrons freeze sequentially when a system follows Bjorken expansion. However, the freeze-out of these strange hadrons appears as common or simultaneous in case of Hubble-like expansion. This is because the number-changing interactions continue until late times for Bjorken expansion as it is slow in nature, due to which inelastic scattering rates of the strange species are greater than the expansion rate of the system. But, in case of the Hubble expansion, the expansion rate is fast; number densities become low quickly as temperature falls sharply, making the mean-free path of strange hadrons suddenly large. This leads to an early freeze-out of the strange species. Here the calculation is microscopic in nature as the interaction cross sections of all species are considered in rate equation.

In principle, different inelastic processes have different thresholds; hence, the freeze-out should always be sequential in nature. But, when the expansion is much faster (e.g., Hubble-like), the mean-free path becomes large (compared to the system dimension) within a short span of time, allowing each species to decouple quickly. The duration is so short that the entire process appears to be simultaneous where all particles appear to have frozen out at the same temperature. However, the sequential nature of freeze-out is prominent and distinguishable in case of a slow expansion (e.g., Bjorken). This sequential nature is visible from the ratio of scattering rate to expansion rate.

The hadronic system considered here is approximately similar to the scenario created at RHIC and LHC. At RHIC and LHC massive strange and nonstrange hadrons are created, which are not considered here, but with less abundances. They should not contribute much to the properties of hadronic medium. Even if the contributions from such massive hadrons and resonances are considered, the conclusions should not change qualitatively. In fact, recent calculation by Alba *et al.* [42] shows that the higher resonances (additional to the list of resonances mentioned in PDG2016+) mildly affect the *chemical freeze-out* temperature, lowering it by a small amount.

In summary, the *chemical freeze-out* dynamics has been analyzed microscopically with both slow (Bjorken) and fast expansion (Hubble-like) scenarios for a multicomponent hadronic fluid. The actual hadronic system produced in relativistic heavy ion collisions will follow a scenario in between these two. Thermal or statistical-hadronization models mostly predict a simultaneous freeze-out of different species which would then mean that the last stage of the fireball or hadronic matter produced at RHIC and LHC follows a fast expansion similar to Hubble-like expansion. Any deviation from a single *chemical freeze-out* temperature may then be attributed to the slower expansion of the system.

In this study we have only discussed *chemical freeze-out*, as the study of *kinetic freeze-out* is far more complex to understand using transport equation. This is because the evolution of momentum distributions is more involved compared to the evolution of particle densities. Hence, it is a separate work to be investigated in the future. The evolution of a particular species after kinetic freeze-out is simple; the particle number density goes as R^{-3} and momentum falls as R^{-1} keeping the total number fixed, where R is the system dimension. Based on the success of the thermal models to fit yield ratios with a single temperature, the answer to the question that whether there is a single *chemical* (T_{ch}) and *kinetic* (T_k) freeze-out temperature, is probably yes, indicating that the system expansion is too fast so that elastic and inelastic scatterings stop suddenly. However, such a conclusion needs a precise modeling of the expansion of the system which requires precise determination of system properties like transport coefficients etc.

[1] B. B. Back *et al.*, Nucl. Phys. **A757**, 28 (2005); J. Adams *et al.*, Nucl. Phys. **A757**, 102 (2005); K. Adcox *et al.*, Nucl. Phys. **A757**, 184 (2005).

[2] *Quarkgluon Plasma: Theoretical Foundations*, edited by J. I. Kapusta, B. Mller, and J. Rafelski (North-Holland, Amsterdam, 2003), ISBN 978-0-444-51110-2.

[3] M. Gyulassy, arXiv:nucl-th/0403032.

[4] Y. Akiba *et al.*, arXiv:1502.02730.

[5] *Melting Hadrons, Boiling Quarks—From Hagedorn Temperature to Ultra-Relativistic Heavy-Ion Collisions at CERN*, edited by J. Rafelski (Springer International Publishing, New York, 2016), https://doi.org/10.1007/978-3-319-17545-4, ISBN 978-3-319-17544-7.

[6] D. Banerjee, J. K. Nayak, and R. Venugopalan, in *The Physics of the QuarkGluon Plasma: Introductory Lectures*, Lecture Notes in Physics, edited by S. Sarkar, H. Satz, and B. Sinha (Springer, Heidelberg, 2010), Vol. 785, pp. 105–137, arXiv:0810.3553, https://doi.org/10.1007/978-3-642-02286-9, ISBN 978-3-642-02285-2.

[7] J. Rafelski, Eur. Phys. J. Special Topics **229** (2020) 1.

[8] R. Venugopalan, J. Phys. G **35**, 104003 (2008).

[9] P. Braun-Munzinger, D. Magestro, K. Redlich, and J. Stachel, Phys. Lett. B **518**, 41 (2001).

[10] A. Andronic, P. Braun-Munzinger, and J. Stachel, Nucl. Phys. **A772**, 167 (2006).

[11] G. Torrieri, Ph.D. thesis, 2004, arXiv: nucl/th-040502.

[12] A. Andronic, P. Braun-Munzinger, and J. Stachel, Phys. Lett. B **673**, 142 (2009); **678**, 516(E) (2009).

[13] S. K. Tiwari, P. K. Srivastava, and C. P. Singh, Phys. Rev. C **85**, 014908 (2012).

[14] A. Andronic, P. Braun-Munzinger, K. Redlich, and J. Stachel, J. Phys. G **38**, 124081 (2011).

[15] S. Chatterjee, R. M. Godbole, and S. Gupta, Phys. Lett. B **727**, 554 (2013).

[16] S. Chatterjee, D. Mishra, B. Mohanty, and S. Samanta, Phys. Rev. C **96**, 054907 (2017).

[17] U. Heinz and G. Kestin, Proc. Sci., CPOD2006 (**2006**) 038 [arXiv:nucl-th/0612105].

[18] S. Takeuchi, K. Murase, T. Hirano, P. Huovinen, and Y. Nara, Phys. Rev. C **92**, 044907 (2015); Nucl. Phys. **A834**, 241C (2010).

[19] P. Dasgupta, R. Chatterjee, and D. K. Srivastava, J. Phys. G **47**, 085101 (2020).

[20] R. Chatterjee, E. S. Frodermann, U. Heinz, and D. K. Srivastava, Phys. Rev. Lett. **96**, 202302 (2006).

[21] C. Ye, P. Mota, J. Li, K. Lin, and W.-L. Qian, Commun. Theor. Phys. **71**, 1281 (2019).

[22] H.-H. Ma, D. Wen, K. Lin, W.-L. Qian, B. Wang, Y. Hama, and T. Kodama, Phys. Rev. C **101**, 024904 (2020).

[23] J. K. Nayak and B. Sinha, Phys. Lett. B **719**, 110 (2013).

[24] G. S. Denicol, C. Gale, S. Jeon, A. Monnai, B. Schenke, and C. Shen, Phys. Rev. C **98**, 034916 (2018).

[25] C. Gale, S. Jeon, and B. Schenke, Int. J. Mod. Phys. A **28**, 1340011 (2013).

[26] P. Koch, B. Muller, and J. Rafelski, Phys. Rep. **142**, 167 (1986).

[27] *The Early Universe*, edited by E. W. Kolb and M. S. Turner (CRC Press, New York, 2018), ISBN-13:978-0201626742.

[28] V. K. Magas, L. P. Csernai, and E. Molnar, Int. J. Mod. Phys. E **16**, 1890 (2007).

[29] F. Grassi, Y. Hama, and T. Kodama, Phys. Lett. B **355**, 9 (1995).

[30] P. F. Kolb and U. Heinz, arXiv:nucl-th/0305084.

[31] D. Teaney, arXiv:nucl-th/0204023

[32] O. Socolowski, Jr., F. Grassi, Y. Hama, and T. Kodama, Phys. Rev. Lett. **93**, 182301 (2004).

[33] L. V. Bravinia *et al.*, *Proc. Sci.*, CORFU2018 (2018) 171.

[34] R. Bellwied, EPJ Web Conf. **171**, 02006 (2018).

[35] S. Bhattacharyya, D. Biswas, S. K. Ghosh, R. Ray, and P. Singha, Phys. Rev. D **101**, 054002 (2020).

[36] S. Gupta, J. K. Nayak, and S. K. Singh, Phys. Rev. D **103**, 054023 (2021).

[37] J. Kapusta and A. Mekjian, Phys. Rev. D **33**, 1304 (1986).

[38] C. M. Ko and L. Xia, Phys. Rev. C **38**, 179 (1988).

[39] P. Gondolo and G. Gelmini, Nucl. Phys. **B360**, 145 (1991).

[40] P. Parotto, M. Bluhm, D. Mroczek, M. Nahrgang, J. Noronha-Hostler, K. Rajagopal, C. Ratti, T. Schäfer, and M. Stephanov, Phys. Rev. C **101**, 034901 (2020).

[41] P. Ghosh, J. K. Nayak, S. K. Singh, and S. Agarwalla, Phys. Rev. D **101**, 094004 (2020).

[42] P. Alba, V. M. Sarti, J. Noronha-Hostler, P. Parotto, I. Portillo-Vazquez, C. Ratti, and J. M. Stafford, Phys. Rev. C **101**, 054905 (2020).